cancers

MDPI

Article

Association Between Circulating CD107a^{+} Natural Killer Cells and Clinical Nodal Stage in Early Breast Cancer: An Exploratory Prospective Biomarker Cohort Study

Ying-Wen Su [1,2,3,4], Sheng-Hsiang Lin [5,6,7], Chi-Hui Hsu [7], Jen-Yu Wang [1,2,8,9], Tzu-Tsen Yu [2], Jie-Jen Lee [1,10], Puo-Wei Wang [2] and Po-Sheng Yang [1,10,*]

1 Department of Medicine, MacKay Medical University, New Taipei City 252005, Taiwan
2 Precision Medicine and Biotechnology Center, Department of Biotechnology Medicine, MacKay Memorial Hospital, Taipei 104217, Taiwan
3 Division of Hematology and Medical Oncology, Department of Internal Medicine, MacKay Memorial Hospital, Taipei 104217, Taiwan
4 Division of Precision Medicine, Department of Biotechnology Medicine, MacKay Memorial Hospital, Taipei 104217, Taiwan
5 Institute of Clinical Medicine, College of Medicine, National Cheng Kung University, Tainan 704302, Taiwan
6 Department of Public Health, College of Medicine, National Cheng Kung University, Tainan 704302, Taiwan
7 Biostatistics Consulting Center, National Cheng Kung University Hospital, College of Medicine, National Cheng Kung University, Tainan 704302, Taiwan
8 Department of Dermatology, MacKay Memorial Hospital, Taipei 104217, Taiwan
9 Department of Cosmetic Applications and Management, MacKay Junior College of Medicine, Nursing and Management, Taipei 112021, Taiwan
10 Department of General Surgery, MacKay Memorial Hospital, Taipei 104217, Taiwan
* Correspondence: psyang.4323@mmh.org.tw

Simple Summary

Doctors currently lack a simple, minimally invasive way to identify which patients with early breast cancer are at higher risk of relapse or worse outcomes. This study examined whether the levels of a specific immune cell in the blood, called an activated natural killer cell, measured before surgery, were linked to more advanced disease, cancer relapse, or death. The researchers also studied tumor tissue to look for genetic patterns that might explain this link. They found that lower blood levels of these activated immune cells were associated with worse outcomes, and a related gene pattern in tumors was linked to survival in a large cancer database. These early results suggest that a simple blood test measuring immune activity could one day help identify higher-risk patients earlier, but larger, well-designed studies are still needed before such a test could be used in everyday clinical practice.

Abstract

Objectives: Minimally invasive biomarkers for risk stratification in early breast cancer are lacking. We examined whether pretreatment circulating natural killer (NK)-cell subsets, specifically CD107a^{+} NK cells, are associated with clinicopathological features and outcomes of early breast cancer and whether tumor transcriptomes reflect NK-cell subset levels. **Materials and Methods:** Circulating NK-cell subsets were quantified by flow cytometry in 94 patients with stages I–III breast cancer prior to surgery and systemic therapy (median follow-up 42.6 months; 10 relapses, 7 deaths). Associations across 12 immune subsets were corrected for multiple comparisons (Benjamini–Hochberg false-discovery rate, FDR). Matched tumor RNA-sequencing ($n = 25$) informed a weighted CD107a-associated tumor-expression score that was examined for an association with survival in TCGA-BRCA ($n = 1096$). **Results:** Low circulating CD107a^{+} NK-cell levels were associated with clinically node-positive disease (cN1–3, raw $p = 0.048$), increased relapse rate ($p = 0.003$),

Check for updates

Academic Editor: Maria Gazouli

Received: 11 September 2026
Revised: 3 November 2026
Accepted: 3 November 2026
Published: 13 November 2026

Copyright: © 2026 by the authors. Licensee MDPI, Basel, Switzerland. This article is an open access article distributed under the terms and conditions of the Creative Commons Attribution (CC BY) license.

and death ($p < 0.001$). Of 96 association tests, only the CD107a$^+$ NK-cell level and overall survival approached significance after FDR correction (q = 0.096); the clinical nodal-stage association did not survive correction (q = 0.93). Exploratory multivariable models were unstable given the few events. Immunoglobulin lambda genes, the dominant contributors to the tumor-expression score, separated survival in TCGA-BRCA (log-rank $p = 0.0096$), confirming a tumor signature rather than validating circulating CD107a$^+$ NK cells as a biomarker. **Conclusions:** Low circulating CD107a$^+$ NK cells were associated with, but do not yet establish, higher-risk early breast cancer. The findings of the present study are hypothesis-generating and do not confirm biomarker status of CD107a$^+$ NK cells in early breast cancer. Prospective, adequately powered, externally validated studies are required before prognostic or therapeutic use.

Keywords: natural killer cells; breast cancer; immune-cell subsets; CD107a$^+$ NK cell; clinical nodal stage; prognosis

1. Introduction

Tumor recurrence following primary treatment for early breast cancer is a major predictor of breast cancer-specific mortality and is a leading cause of cancer deaths worldwide [1,2]. The immune system eliminates residual cancer cells; and recurrence risk rises when tumor cells evade antitumor immune responses.

Natural killer (NK) cells are cytotoxic innate lymphoid cells that recognize and eliminate cancer cells without prior antigen sensitization [3], thereby lysing transformed cells, promoting the infiltration of other cytotoxic immune cells, and responding to stress-induced ligands on cancer cells [4]. NK cells are defined by CD56 overexpression and the absence of the CD3–T-cell receptor complex [5] and comprise a predominant cytotoxic CD56^{dim} CD16$^+$ subset and a smaller cytokine-producing CD56^{bright} CD16$^{dim/-}$ subset [6,7]. On degranulation, CD107a (LAMP-1), a lysosomal-associated membrane protein, is transiently expressed at the cell surface and serves as an activation marker [8]. Unlike lineage or abundance markers, CD107a reflects functional degranulation: patients with similar total NK-cell counts can differ substantially in cytotoxic engagement, which a simple NK-cell count cannot capture. NK cytotoxicity is governed by the balance between activating cells (NKp30/CD337, DNAM-1/CD226, 2B4/CD244, NKG2D/CD314) and inhibitors (killer immunoglobulin-like receptors, NKG2A/CD159a) [9].

Circulating immune cells may provide an alternative approach for assessing host–tumor immunity in early-stage cancer before an immunosuppressive microenvironment is established [10]. Pretreatment circulating NK cells or lymphocyte levels correlate modestly with tumor-infiltrating lymphocytes (TILs) [11], but tumor-derived immunosuppressive proteins reduce degranulation of circulating NK cells and alter T/B-cell profiles [12]. Circulating immunophenotype should therefore be interpreted as a distinct, complementary compartment of host anti-tumor immunity, not as a surrogate for tumor-infiltrating immunity. Reports on circulating NK-cell subsets in breast cancer are inconsistent: mature, cytotoxic subsets are associated with improved overall survival (OS) in triple-negative disease [13], immature or non-cytotoxic NK cells are predominant in advanced disease [14], and some studies found no associations between NK cells and cancer stage [15]. Therefore, the prognostic value of specific NK-cell subsets and their associations with tumor-derived protein expression remain unresolved.

Because tumor-derived factors can impair the cytotoxic function of circulating NK cells without necessarily reducing their numbers [7,12], we hypothesized that a functional marker such as CD107a might capture differences in host anti-tumor immunity that total NK-cell

counts or receptor-defined subsets do not. This prospective cohort study therefore examined associations between pretreatment circulating NK-cell subsets, including CD107a$^+$ NK cells, and clinical nodal stage, relapse and survival in early breast cancer. We also explored whether tumor transcriptomes reflect circulating NK-subset levels, as a first step towards identifying candidate biomarkers.

2. Methods

2.1. Ethical Considerations

This study was conducted in accordance with the Declaration of Helsinki. The study protocol was reviewed and approved by the Institutional Review Board of MacKay Memorial Hospital (Approval numbers: 18MMHIS050, Approval date: 22 August 2018; Approval numbers: 21MMHIS069e, Approval date: 20 April 2021). Signed informed consent was received from all patients.

2.2. Study Design and Participants

Figure 1 summarizes the study population selection and CONSORT-style patient flow. This single-center, prospective observational cohort study enrolled 96 patients between 1 September 2018 and 30 September 2022. Eligible patients had histologically confirmed invasive breast cancer, clinical stage I–III at diagnosis, no prior anticancer treatment at enrollment, and the capacity to provide informed consent. Two patients who did not complete the predetermined standard treatment were excluded, leaving 94 patients for flow cytometric analysis. Pretreatment tumor RNA-sequencing required separate consent and sufficient residual tissue. Twenty-seven patients consented, and two samples failed quality control, leaving 25 patients (26.6% of 94) for analysis (Table S10). This subset was therefore not a random sample of the cohort.

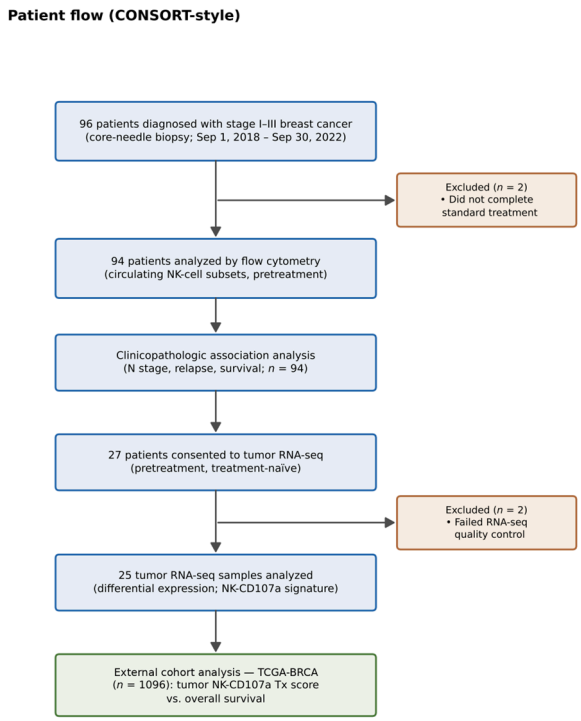


Figure 1. Study population selection and CONSORT-style patient flow.

Baseline evaluations (complete blood count, differential white blood count, NK subtype analysis) preceded anticancer treatment. All patients underwent surgery with adjuvant

or neoadjuvant chemotherapy; HER2-positive patients received trastuzumab concurrently with adjuvant or neoadjuvant chemotherapy, followed by trastuzumab monotherapy every 3 weeks for up to 1 year. Patients with hormone receptor (HR)-positive tumors received adjuvant endocrine treatment until relapse or for up to 10 years, whichever occurred first. Clinical and pathological data were obtained by chart review, including demographic data, pathology type, tumor histological grade, tumor–node–metastasis (TNM) stage, estrogen receptor (ER), progesterone receptor (PR), HER2, Ki67 proliferation index, date of relapse, and death. TNM staging followed the American Joint Committee on Cancer (AJCC) Cancer Staging Manual, 8th edition (2017) [16]. Patients were followed until death or 30 September 2024.

2.3. Flow Cytometry

Pretreatment circulating NK-cell subsets were quantified by flow cytometry, as previously described [6]. The gating strategy and representative dot plots for NK-cell subsets are shown in Figure S1. Peripheral blood mononuclear cell (PBMC) suspensions were stained with the following antibodies: fluorescein isothiocyanate (FITC)–CD3, peridinin–chlorophyll-protein/cyanine 5.5 (PerCP/Cy5.5)–CD16, and phycoerythrin (PE)–CD56 (NK-cell identification). FITC–CD4, PE–CD19, and PerCP-CD8 were stained in separate tubes for lymphocyte subset identification. NK-cell receptors were detected with allophycocyanin (APC)–CD158 (KIR2D L1/S1/S3/S5), APC–CD158e1 (KIR3DL1), APC–CD159a (NKG2A), APC–CD226 (DNAM-1), APC–CD244 (2B4), APC–CD314 (NKG2D), and Alexa Fluor 647–CD337 (NKp30) (all BioLegend, San Diego, CA, USA), and eFluor660-CD107a (eBioscience, San Diego, CA, USA). Briefly, peripheral blood was collected in EDTA tubes (BD Vacutainer, BD Biosciences, Franklin Lakes, NJ, USA) before any anticancer treatment, and peripheral blood mononuclear cells (PBMCs) were isolated by density-gradient centrifugation (Ficoll-Paque PLUS, Cytiva, Uppsala, Sweden) within 6 h of collection. For each tube, 5×10^5 PBMCs were stained with the antibody combination for 30 min at 4 °C in the dark, washed, fixed with 4% paraformaldehyde for 20 min, washed twice with phosphate-buffered saline (PBS) and acquired on a BD FACSCalibur (BD Biosciences, Franklin Lakes, NJ, USA) with CellQuest Pro software recording at least 10,000 lymphocyte-gated events per tube. Because the BD FACSCalibur has a limited number of fluorescence detectors and the APC-region fluorochromes (APC, Alexa Fluor 647, and eFluor 660) overlap spectrally, each of these markers was acquired in a separate tube together with CD3, CD56 and CD16, so that only one APC-region fluorochrome was present per tube. Co-expression of different receptors on the same cells could therefore not be assessed. NK cells were defined as $CD3^{-}CD56^{+}$ cells within the lymphocyte gate (forward/side scatter) and divided into CD56dim CD16bright and CD56bright CD16dim subsets. Unstained cells and single-stained cells were used to set compensation and the positivity thresholds. CD107a (LAMP-1) was measured by direct surface staining of unstimulated PBMCs and therefore reflects baseline surface expression, not stimulation-induced degranulation. A doublet-exclusion gate and a viability dye were not used (see Strengths and Limitations).

2.4. RNA-Sequencing and Differential Expression

RNA extraction, library preparation, cluster generation, and sequencing were performed on Illumina HiSeq2500 (Illumina, San Diego, CA, USA) using the SureSelect XT HS2 mRNA Library Preparation kit (Agilent Technologies, Santa Clara, CA, USA), as previously described [17]. Two of the 27 tumor samples were excluded from subsequent analyses because they did not meet the RNA quality requirements, with either an insufficient RNA input amount (<10 ng) or an RNA integrity number (RIN) < 8. FASTQ files were generated from the sequencing data using Illumina's basecalling program bcl2fastq v2.20. Raw

reads were subjected to quality control using fastp v1.3.2 and FastQC v0.12.1 and were quality-trimmed and filtered using Trimmomatic v0.36 (PMID: 24695405) (ILLUMINACLIP:1:10:4, LEADING:20, TRAILING:13, SLIDINGWINDOW:5:20, MINLEN:30), with adapter sequences and low-quality bases removed. A median of 68.70 M reads (range, 34.88–155.62 M) passed filtering. The filtered reads were aligned to the GRCh38.p13 reference genome using HISAT2 [18]. An average of 66.58 million clean reads per sample (range, 32.54–153.14 million) were retained, with a mean alignment rate of 97.56%. Gene expression was quantified with StringTie v2.1.4 [19], normalized to transcripts per million (TPM), and subsequently log2-transformed as log2(TPM + 1) for differential expression analysis.

To identify differentially expressed genes (DEGs) associated with circulating NK-cell subset levels ($CD107a^+$, $CD226^+$, $CD244^+$, $CD314^+$, $CD337^+$, $CD158^+$, $CD158e1^+$, and $CD159a^+$ NK-cells) as well as B ($CD19^+$) and T ($CD4^+$ and $CD8^+$) lymphocytes, the transformed expression data from 25 breast tumor samples were analyzed using the limma R package v3.62.2 [20]. Lowly expressed genes were filtered, and p values were adjusted for multiple testing using the Benjamini–Hochberg method. Batch effects were assessed by principal component analysis and PERMANOVA. Samples did not cluster by sequencing run or library preparation date (PERMANOVA $p = 0.38$ and $p = 0.42$, respectively), and no principal component was associated with either variable (Supplementary Figure S2). Therefore, no batch correction was applied [21]. Genes with missing gene symbols were excluded, and the remaining genes were annotated as upregulated ($\log_2$foldchange [FC] > 1 and $p.$ adj < 0.05), downregulated ($\log_2$FC < -1 and $p.$ adj < 0.05), or not significant. Gene set enrichment analysis (GSEA) and over-representation analysis used clusterProfiler R package v4.14.4 with Gene Ontology (GO), Kyoto Encyclopedia of Genes and Genomes (KEGG), Disease Ontology, and Reactome pathways [22]. Given the small discovery set ($n = 25$, with subtype subgroups as small as $n = 3$), these transcriptomic analyses were considered exploratory and hypothesis-generating.

2.5. Public Database Acquisition and Construction of a Prognostic Model

To build a compact, reproducible signature from a small discovery cohort for testing in a much larger independent cohort, we used the top five upregulated and downregulated genes (by absolute fold change) from the $CD107a^+$ NK-cell comparison as the signature. A weighted tumor expression score (NK-CD107a Tx score) was computed for each Cancer Genome Atlas Breast Carcinoma Project (TCGA-BRCA) patient ($n = 1096$) using the $\log_2$FC of each signature gene as its weight, and patients were split at the median for Kaplan–Meier and Cox analyses. TCGA does not contain circulating NK-cell subset measurements; this analysis therefore confirms a tumor-expression signature and does not validate the NK-cell subset as a circulating biomarker. Sensitivity analyses varying signature size and using an immunoglobulin-gene-only score are planned (see Strengths and Limitations).

2.6. Statistical Analysis

No formal a priori sample size or power calculation was performed. This was an exploratory, hypothesis-generating biomarker cohort based on feasible single-center enrollment over a defined period rather than a target effect size. Pretreatment NK-cell subsets were divided into two distinct parts of the relevant denominator labeled Low (<20%) versus Not Low (≥20%); denominators are footnoted per table (NK-cell receptor subsets as a proportion of $CD3^-CD56^+$ NK cells; total NK cells as a proportion of lymphocytes; T/B lymphocytes as a proportion of total blood cells).

The 20% cutoff was selected using a minimum-p-value approach [23] because data-driven cutoff selection inflates the Type I error rate, which is noted as a limitation. Associations between categorical pretreatment NK data and age, clinical TNM staging, relapse,

and death were assessed. Continuous variables are presented as the median (interquartile range, IQR) and compared using the Mann–Whitney U test, except for the variables in Table 1, which are reported as the median (minimum–maximum). Categorical variables are presented as numbers (percentages) and were analyzed using the Chi-square (χ^2) or Fisher's exact test, with Cramer's V for effect size. Because 12 immune-cell subsets were tested against multiple clinicopathologic and outcome variables (96 association tests in total; 72 within the clinicopathologic family), *p*-values were adjusted for multiple comparisons using the Benjamini–Hochberg false-discovery-rate (FDR) method, and adjusted (q) values are reported alongside raw *p*-values. Significant NK-cell subset data were further analyzed using multivariate Cox regression, adjusted for clinicopathological variables (age, T stage, and N stage). Because this study was not powered for the relapse and survival endpoints, and only 10 relapses and 7 deaths occurred (below the conventional ≥ 10 events-per-variable threshold; see Strengths and Limitations), these multivariable models and the resulting hazard ratios are exploratory, not confirmatory. All statistical analyses were performed using SAS version 9.4 (SAS Institute Inc., Cary, NC, USA). A two-sided $p < 0.05$ was established as statistical significance unless otherwise specified. For analyses involving multiple comparisons, statistical significance was determined using Benjamini–Hochberg FDR-adjusted q-values < 0.1, while raw *p*-values are also reported.

Table 1. Patients' demographic and clinical characteristics (94 patients).

	Value
Age, median (range)	53.1 (range: 33.8–76.3)
Stage I/II/III	22 (23.4%)/60 (63.8%)/12 (12.8%)
Clinical nodal stage cN0/cN1–3	51 (54.3%)/43 (45.7%)
Tumor subtypes HR+/HER2-/HER2+/TNBC	48 (51.1%)/28 (29.8%)/18 (19.1%)
Adjuvant treatment Neoadjuvant/adjuvant chemotherapy	32 (34.0%)/62 (66.0%)
Relapse/death	10/7
$CD3^-CD56^+$ NK-cell percentage *, median (IQR)	17.0% (11.3–25.1%)
$CD107a^+$ percentage ¥, median (IQR)	56.4% (24.4–69.6%)

* The proportion of the total lymphocyte count; ¥ the proportion of $CD3^-CD56^+$ NK-cell count; Abbreviations: HR, hormone receptor; HER2, human epidermal growth factor receptor 2; IQR: interquartile range; TNBC: triple-negative breast cancer.

3. Results

3.1. Associations Between NK-Cell Subsets and Clinical Parameters

The study cohort comprised 94 patients with stages I–III breast cancer (median age 53.1 years; 63.8% stage II; 51.1% HR-positive/HER2-negative; 34.0% neoadjuvant chemotherapy). The median follow-up was 42.6 months (IQR 32.8–53.2); 10 patients relapsed, and 7 died (Table 1).

Each NK-cell subset was tested against age, clinical T and N stage, tumor subtype, HR status, HER2 expression, relapse and survival (Supplementary Tables S1–S8). Patients with low circulating $CD107a^+$ NK cells were more likely to have clinically node-positive disease (cN1–3; Cramer's V = 0.204, raw $p = 0.048$, χ^2 test) (Table S3). Patients with low levels of inhibitory $CD158e1^+$ (KIR3DL1) NK cells were significantly younger (50.82 vs. 57.52 years, $p = 0.048$, Pearson correlation test) (Table S1). No associations were found

between NK cells and clinical T stage, subtype, or HR/HER2 status (Tables S1–S6). Patients who relapsed had greater nodal involvement at diagnosis (N1–3: 80% vs. 41.7%, Cramer's V = 0.237, raw $p = 0.04$, Fisher's Exact test) and lower levels of CD107a$^+$ NK cells (60% vs. 14.3%, Cramer's V = 0.358, raw $p = 0.003$, Fisher's exact test) (Table S7). Patients with low levels of circulating CD107a$^+$ NK cells had higher mortality than those with higher CD107a$^+$ NK-cell levels (85.7% vs. 13.8%, Cramer's V = 0.480, raw $p < 0.001$, Fisher's exact test) (Table S8).

3.2. Multiple Comparisons Correction

Benjamini–Hochberg FDR correction was applied to the 96 association tests (12 immune subsets × 8 clinicopathologic/outcome comparisons) (Table S9). Only the CD107a–overall-survival association approached significance after FDR correction (raw $p < 0.001$, q = 0.096) and the CD107a–relapse association gave q = 0.144. The CD107a–clinical-nodal-stage association (raw $p = 0.048$) did not survive correction (q = 0.93), nor did the CD158e1–age association (q = 0.93) (Table 2), suggesting that the nodal-stage association is consistent with a chance finding under this many comparisons and should be interpreted as exploratory; the association of low CD107a$^+$ NK cells with poorer survival was the most robust signal in the dataset.

Table 2. Associations between NK-cell subsets and clinical–pathologic parameters.

Association (Immune Subset × Variables)	Cramer's V	Raw p	BH-Adj. p (q)	Survives FDR (q < 0.10)
CD107a-Low × Overall survival	0.480	<0.001	0.096	Yes
CD107a-Low × Relapse	0.358	0.003	0.144	No
CD107a-Low × Clinical nodal stage	0.204	0.048	0.93	No
CD158e1 (KIR3DL1)-Low × age	-	0.048	0.93	No

NK cells: natural killer cells; Low: defined as <20% of CD3$^-$CD56$^+$ NK-cell count; 96 tests total: 12 NK subsets × 8 clinicopathologic outcome comparisons; BH-adj. p (q): False discovery rate (FDR)-adjusted p-value calculated using the Benjamini–Hochberg procedure or Benjamini–Hochberg q value.

3.3. Circulating CD107a$^+$ NK Cells, Tumor Transcriptome and Outcomes

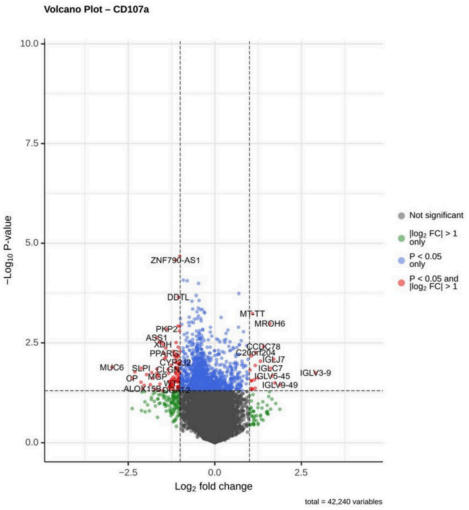
Comparison of tumor transcriptomes and circulating CD107a$^+$ NK-cell levels identified the top differentially expressed genes (Figure 2). The five most upregulated were immunoglobulin lambda genes (*IGLV3-9*, *IGLV9-49*, *IGLV2-18*, *IGLV5-45*, *IGLJ7*); the five most downregulated were *MUC6*, *CP*, *CYP4F8*, *LBP* and *SLPI*. Over-representation analysis showed enrichment of lipid biosynthetic process, blood vessel morphogenesis, cellular response to growth factor, and oxidoreductase activity gene sets in tumors with suppressed circulating CD107a$^+$ NK cells (Figure 2C, left). KEGG gene-set enrichment analyses linked reduced circulating CD107a$^+$ NK cells to MAPK, TNF, IL-17 and PPAR signaling (Figure 2C, right). A detailed list of the top 10 DEGs for each NK-cell subset is shown in Figures S3–S7. These transcriptomic associations are exploratory and hypothesis-generating; they were derived from 25 tumors and do not establish causation (see Section 4).

(A)

ensembl	symbol	log2FoldChange	p_value	Significance
ENSG00000211670	*IGLV3-9*	2.906407	1.77×10^{-2}	Upregulated
ENSG00000223350	*IGLV9-49*	1.880092	3.57×10^{-2}	Upregulated
ENSG00000211664	*IGLV2-18*	1.730799	3.19×10^{-2}	Upregulated
ENSG00000211684	*IGLJ7*	1.701235	8.18×10^{-3}	Upregulated
ENSG00000211650	*IGLV5-45*	1.657538	2.13×10^{-2}	Upregulated
ENSG00000211685	*IGLC7*	1.608790	1.36×10^{-2}	Upregulated
ENSG00000204839	*MROH6*	1.588984	1.03×10^{-3}	Upregulated
ENSG00000162004	*CCDC78*	1.402248	3.92×10^{-3}	Upregulated
ENSG00000188883	*KLRG2*	1.317695	9.10×10^{-3}	Upregulated
ENSG00000103485	*QPRT*	1.242580	2.38×10^{-2}	Upregulated

ensembl	symbol	log2FoldChange	p_value	Significance
ENSG00000184956	*MUC6*	−2.972158	1.29×10^{-2}	Downregulated
ENSG00000047457	*CP*	−2.392214	2.45×10^{-2}	Downregulated
ENSG00000186526	*CYP4F8*	−2.308354	1.68×10^{-2}	Downregulated
ENSG00000129988	*LBP*	−2.131840	3.06×10^{-2}	Downregulated
ENSG00000124107	*SLPI*	−2.125097	1.35×10^{-2}	Downregulated
ENSG00000179593	*ALOX15B*	−2.088322	4.47×10^{-2}	Downregulated
ENSG00000012223	*LTF*	−2.039867	3.67×10^{-2}	Downregulated
ENSG00000196136	*SERPINA3*	−1.970717	1.96×10^{-2}	Downregulated
ENSG00000240216	*CPHL1P*	−1.860515	3.53×10^{-2}	Downregulated
ENSG00000171236	*LRG1*	−1.821605	1.75×10^{-2}	Downregulated

(B)



(C)

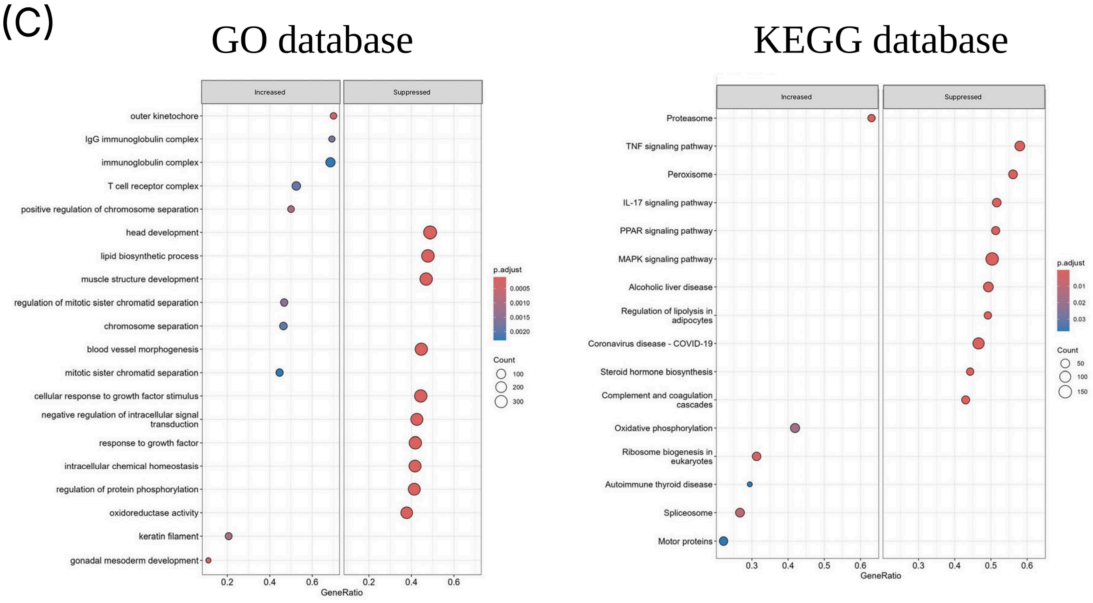


Figure 2. Differential tumor gene expression by circulating CD107a$^+$ NK-cell levels. (**A**) Top 10 differentially expressed genes; (**B**) volcano plot; (**C**) gene-set enrichment (GO/KEGG) linking reduced circulating CD107a$^+$ NK cells to MAPK, TNF, IL-17 and PPAR signaling.

3.4. Tumor Expression Score for Circulating CD107a$^+$ NK Cells Is Associated with Survival Outcome

The NK-CD107a Tx score used the top five upregulated (*IGLV3-9*, *IGLV9-49*, *IGLV2-18*, *IGLJ7*, and *IGLV5-45*) and downregulated genes (*MUC6*, *CP*, *CYP4F8*, *LBP*, and *SLPI*) ranked by absolute FC (Figure 2), applied as a weighted sum in TCGA-BRCA ($n = 1096$). Selecting a small, fixed number of the most differentially expressed genes by fold change is a pragmatic way to build a compact, reproducible signature from a small discovery cohort ($n = 25$) for testing in a much larger cohort (TCGA-BRCA, $n = 1096$), as with the 14-gene B-cell/immunoglobulin signature [24]. Whether the signal is specific to CD107a$^+$ NK-cell biology still requires an immunoglobulin-gene-only sensitivity analysis and cross-validated

discrimination, which are planned (see Section 4). Patients with low NK-CD107a Tx scores had worse survival ($p = 0.0096$ by log-rank test; Figure 3).

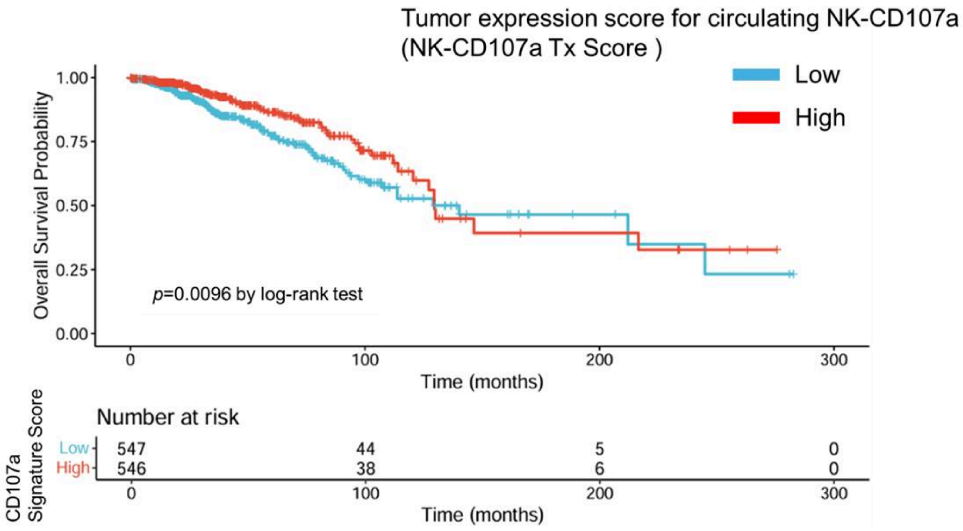


Figure 3. Kaplan–Meier survival curves comparing high- and low-tumor expression scores for CD107a$^+$ NK cells (NK-CD107a Tx score) in each patient group analyzed using the log-rank test.

In exploratory multivariable Cox models, low circulating CD107a$^+$ NK cells were associated with relapse (adjusted HR = 4.49, 95% CI: 1.19–16.87, $p = 0.026$; Table 3) and mortality (adjusted HR = 16.15, 95% CI: 1.72–151.76, $p = 0.015$; Table 4). These HRs are unstable given only 10 relapses and 7 deaths (see Section Strengths and Limitations) and are reported as exploratory. The TCGA analysis confirms the tumor-expression signature and does not validate circulating NK cells as a biomarker.

Table 3. Crude and adjusted HRs for relapse according to clinical parameters and NK-cell subsets.

	Factors	Crude HR (95% CI)	*p*-Value	Adjusted HR (95% CI)	*p*-Value
	Age	1.02 (0.96–1.08)	0.510	1.03 (0.97–1.10)	0.319
	T2–4 vs. T1	1.64 (0.42–6.35)	0.475	1.75 (0.44–6.95)	0.426
	N1–3 vs. N0	4.97 (1.05–23.41)	0.043 *	3.25 (0.64–16.41)	0.154
NK with activating surface markers	NK107a: Low vs. Not Low	5.69 (1.59–20.38)	0.008 *	4.49 (1.19–16.87)	0.026 *
	CD226 (DNAM-1): Low vs. Not Low	0.47 (0.06–3.75)	0.479		
	CD244 (2B4): Low vs. Not Low	0.97 (0.21–4.59)	0.973		
	CD314 (NKG2D): Low vs. Not Low	1.21 (0.26–5.74)	0.808		
	CD337 (NKp30): Low vs. Not Low	1.19 (0.25–5.62)	0.828		
NK with inhibitory surface markers	CD158 (KIR2DL1): Low vs. Not Low	1.11 (0.24–5.25)	0.893		
	CD158e1 (KIR3DL1): Low vs. Not Low	2.06 (0.53–7.97)	0.296		
	CD159a (NKG2A): Low vs. Not Low	2.20 (0.56–8.59)	0.257		
T lymphocytes	CD4: Low vs. Not Low	1.05 (0.22–4.97)	0.948		
	CD8: Low vs. Not Low	0.54 (0.07–4.26)	0.555		
B lymphocytes	CD19: Low vs. Not Low	1.99 (0.54–7.26)	0.300		

* $p < 0.05$; Abbreviations: HR, hazard ratio; CI, confidence interval; NK, natural killer.

Table 4. Crude and adjusted HRs for mortality stratified by clinical parameters and NK-cell subsets.

	Factors	Crude HR (95% CI)	*p*-Value	Adjusted HR (95% CI)	*p*-Value
	Age	1.02 (0.95–1.10)	0.589	1.03 (0.95–1.12)	0.474
	T2–4 vs. T1	1.13 (0.25–5.07)	0.875	1.63 (0.35–7.54)	0.535
	N1–3 vs. N0	2.78 (0.54–14.37)	0.222	1.12 (0.19–6.44)	0.902
NK cells with activating surface markers	NK107a: Low vs. Not Low	15.63 (1.84–132.71)	0.012 *	16.15 (1.72–151.76)	0.015 *
	CD226 (DNAM-1): Low vs. Not Low	1.01 (0.12–8.70)	0.994		
	CD244 (2B4): Low vs. Not Low	0.58 (0.07–4.87)	0.615		
	CD314 (NKG2D): Low vs. Not Low	1.02 (0.12–8.63)	0.982		
	CD337 (NKp30): Low vs. Not Low	2.04 (0.39–10.57)	0.398		
NK cells with inhibitory surface markers	CD158 (KIR2DL1): Low vs. Not Low	2.32 (0.44–12.25)	0.321		
	CD158e1 (KIR3DL1): Low vs. Not Low	1.82 (0.35–9.42)	0.475		
	CD159a (NKG2A): Low vs. Not Low	3.75 (0.83–16.89)	0.085		
T lymphocytes	CD4: Low vs. Not Low	1.91 (0.37–9.90)	0.442		
	CD8: Low vs. Not Low	0.92 (0.11–7.76)	0.939		
B lymphocytes	CD19: Low vs. Not Low	0.65 (0.11–3.65)	0.623		

* $p < 0.05$; Abbreviations: HR, hazard ratio; CI, confidence interval; NK cells, natural killer cells.

4. Discussion

In this exploratory prospective prognostic tumor marker cohort study, low circulating CD107a$^+$ NK cells were associated with greater clinical nodal stage and higher rates of relapse and mortality, suggesting a role for innate immunity in tumor progression. After correction for multiple comparisons, survival was the most robust association, whereas the association with nodal stage did not survive and is regarded as hypothesis-generating. Matched tumor RNA-sequencing linked reduced circulating CD107a$^+$ NK cells to immunoglobulin expression and to MAPK/TNF pathway enrichment, and a tumor-expression score derived from these genes was consistent with survival in TCGA-BRCA.

CD107a, a lysosomal-associated membrane protein expressed on the NK-cell surface upon target recognition, is a recognized marker of NK activation [25]. As detailed in the Section 2, CD107a positivity in this study was assessed by direct staining of unstimulated PBMCs and therefore reflects baseline, spontaneous NK-cell activation in vivo rather than maximal degranulation capacity after ex vivo restimulation—a distinction relevant to interpreting the relatively low proportion of CD107a-positive cells observed at rest. The tumor microenvironment and host immunity are increasingly central to breast cancer prognosis. Immune checkpoint inhibitors (ICIs) in chemotherapy are standard for early-stage TNBC [26] and show benefits in high-risk, early-stage HR-positive/or HER2-negative breast cancer [27,28]. Beyond programmed death-ligand 1 (PD-L1), high TIL levels, particularly CD8$^+$ lymphocytes, are associated with better immunotherapy response and prognosis [29,30]. However, stromal TILs are limited by interobserver variability, lack of a universal cutoff, tumor heterogeneity, and lack of functional resolution [12,31] and are generally low in most early-stage tumors [26,32–35]. So, a blood-based measure of host anti-tumor immunity would have substantial practical value. Circulating immune cells may thus offer a complementary, minimally invasive approach to assessing host–tumor immunity in early breast cancer.

Among all subsets tested, only low circulating CD107a+ NK cells were associated with clinical aggressiveness and relapse. Many NK-cell receptors have overlapping, combined functions, so loss or gain of one receptor may be compensated for by others, and several are broadly expressed across inflammatory conditions and may lack cancer specificity [36], possibly explaining the lack of association with other NK-cell subsets.

The TCGA-BRCA analysis confirmed a tumor gene-expression score and did not validate circulating CD107a+ NK cells as a biomarker, which TCGA does not measure. The inferential chain (blood NK activity → 25-sample tumor DEG signature → TCGA survival → back to circulating NK biology) is indirect and partly circular. Moreover, the top five upregulated signature genes are all immunoglobulin lambda genes (*IGLV*/*IGLJ*). A B-cell/immunoglobulin signature is already an established prognostic marker in breast cancer, independent of NK-cell biology—for example, a 14-gene B-cell/immunoglobulin signature correlates with OS independent of subtype, stage, or nodal status [24,37], suggesting that the TCGA survival separation reiterates this known immunoglobulin signal rather than reflecting CD107a$^+$ NK-cell activity specifically. An immunoglobulin-gene-only sensitivity analysis and cross-validated discrimination are needed to resolve this, and these analyses are planned as future work (see Strengths and Limitations).

The immunoglobulin and pathway findings are associations with the CD107a-defined groups and do not demonstrate biological causation. The following interpretations of possible underlying mechanisms are derived from over-representation/GSEA on 25 tumors without functional or protein-level validation and without single-patient association with the circulating CD107a$^+$ phenotype and are suggested only as hypotheses, not as established mechanisms. Chronic TNF exposure reduces NK-cell cytotoxic efficiency and promotes immune exhaustion [38], and IL-17-enriched microenvironments recruit myeloid-derived suppressor cells that impair NK-cell function [39,40]. MAPK signaling promotes proliferation and immunosuppressive cytokine release [41], and PPAR signaling (i.e., crosstalk with MAPK) integrates lipid/glucose metabolism with inflammation to shape the tumor microenvironment and immune-cell balance [42–44]. Tumor-derived immunoglobulins have been reported to downregulate NK-cell cytotoxicity in advanced-disease or in vitro models [45], whereas in early-stage tumors, immunoglobulin-high status has been associated with tertiary lymphoid structures and B/T-cell polyclonality [37]. How tumor-derived immunoglobulins interact with systemic CD107a$^+$ NK-cell responses is unknown.

Strengths and Limitations

The strengths of the present study include the prospective pretreatment sampling before surgery and systemic therapy, integration of the circulating immunophenotype with matched tumor transcriptomes, and correction for multiple comparisons.

Nevertheless, this study has several limitations. First, the cohort was small and heterogeneous and had very few events (10 relapses, 7 deaths); the results of the multivariable Cox models violate the ≥10 events-per-variable rule, and the mortality HR (16.15; 95% CI 1.72–151.76) was severely unstable, likely reflecting near-separation. Therefore, the results are not interpretable as reliable effect sizes and are reported as exploratory; Firth's penalized regression with minimal adjustment is planned to address these issues. Second, the key association between the NK cells and the clinical nodal stage was weak (Cramer's V 0.204) and did not survive multiple comparisons correction ($q = 0.93$), so a Type I (false-positive) finding cannot be excluded. Third, the <20% cutoff was chosen by a minimum-*p*-value approach, increasing the Type I error rate unless corrected. Fourth, the DEG signature was derived from only 25 tumors using a fixed set of the five most upregulated and five most downregulated genes (selected by fold change as a pragmatic approach to obtaining a compact, reproducible signature), weighted by discovery-cohort $\log_2$FC, which risks overfitting.

Because the top genes were all immunoglobulin lambda genes, the score may reflect the known B-cell/immunoglobulin signal rather than CD107a$^+$ NK-cell biology. Sensitivity analyses varying signature size and using an immunoglobulin-gene-only score, together with cross-validated discrimination, are planned. Fifth, the multivariable models were adjusted only for age, T stage, and N stage. Molecular subtype and treatment modality could not be added given the low number of events, so residual confounding cannot be excluded. Baseline characteristics by CD107a group are compared descriptively in Supplementary Table S11. In addition, aging shifts the NK-cell composition toward KIR-expressing "mature" subsets, and older patients may show reduced CD107a$^+$ responses [46,47]. Younger patients in the present study cohort had lower CD158e1$^+$ (but not CD107a$^+$) NK cells, so residual age confounding cannot be excluded. Sixth, there was no independent external clinical validation cohort; the TCGA-BRCA analysis tests only the tumor-expression signature and does not validate circulating CD107a$^+$ NK cells as a biomarker. Seventh, only NK-cell phenotype and the surface marker CD107a (LAMP-1) were measured; CD107a was measured on unstimulated cells and therefore reflects baseline surface expression rather than stimulation-induced degranulation, and no functional NK-cell cytotoxicity (tumor-cell killing) assays were performed, so functional competence was not directly assessed. Eighth, the flow cytometry data were acquired on an older BD FACSCalibur without a doublet-exclusion gate or viability dye, and the original area/width parameters are no longer available. Positivity thresholds were set with unstained and single-stained controls, not fluorescence-minus-one or isotype controls; marker percentages are therefore descriptive. Ninth, the 25 patients who underwent RNA-sequencing were a self-selected subset of the 94-patient cohort (separate consent and adequate tumor tissue were required) rather than a random subsample, so selection bias cannot be excluded. Larger, prospective, adequately powered studies are required to confirm the hypothesis-generating findings of this study.

5. Conclusions

In this exploratory cohort, low pretreatment levels of circulating CD107a$^+$ NK cells were associated with poorer overall survival, the only association that remained after correction for multiple comparisons, and with higher relapse rates and node-positive disease before correction. These findings show an association; they do not establish CD107a$^+$ NK cells as a prognostic biomarker. Given the small number of events and the data-derived cutoff, they should be regarded as hypothesis-generating. Confirmation is needed in larger, multicenter, prospective cohorts using standardized flow cytometric methodology and a predefined (rather than data-derived) CD107a$^+$ threshold before any prognostic or therapeutic application.

Supplementary Materials: The following supporting information can be downloaded at: https://www.mdpi.com/article/10.3390/cancers18223633/s1, Table S1. Correlation between circulating NK subsets and age; Table S2. Correlation between circulating NK subsets and clinical T stage; Table S3. Correlation between circulating NK subsets and clinical N stage; Table S4. Correlation between circulating NK subsets and tumor subtype; Table S5. Correlation between circulating NK subsets and hormone receptor status; Table S6. Correlation between circulating NK subsets and HER2 status; Table S7. Correlation between circulating NK subsets and relapse; Table S8. Correlation between circulating NK subsets and survival status; Table S9. Multiple comparisons correction across all 96 association tests; Table S10. Characteristics of the RNA-sequencing subcohort ($n = 25$); Table S11. Baseline characteristics of patients with Low versus Not Low circulating CD107a$^+$ NK cells; Figure S1. Flow cytometry gating strategy and representative plots; Figure S2. Assessment of batch effects in the RNA-sequencing data; Figure S3. Top 10 differentially expressed genes and volcano plots for circulating CD226(DNAM1) NK (A,B) and CD244(2B4) NK (C,D) cells; Figure S4. Top

10 differentially expressed genes and volcano plots for circulating CD314(NKG2D) NK (A,B) and CD337(NKp30) NK (C,D) cells; Figure S5. Top 10 differentially expressed genes and volcano plots for circulating CD158(KIR2DL1) NK (A,B) and CD158e1(KIR3DL1) NK (C,D) cells; Figure S6. Top 10 differentially expressed genes and volcano plots for circulating CD159a(NKG2A) NK (A,B) and $CD19^+$ B (C,D) cells; Figure S7. Top 10 differentially expressed genes and volcano plots for circulating $CD4^+$ T (A,B) and $CD8^+$ T (C,D) cells.

Author Contributions: Y.-W.S.: Conceptualization, Funding acquisition, Methodology, Writing—original draft, Writing—reviewing and editing. S.-H.L. and C.-H.H.: Data curation, Formal analysis, Writing—reviewing and editing. J.-Y.W.: Methodology, Writing—original draft. T.-T.Y. and P.-W.W.: Data curation, Methodology, Visualization, Writing—original draft. J.-J.L.: Funding acquisition, Investigation, Writing—reviewing and editing. P.-S.Y.: Funding acquisition, Investigation, Supervision, Writing—reviewing and editing. All authors have read and agreed to the published version of the manuscript.

Funding: This work was supported by the MacKay Memorial Hospital [grant numbers MMH-102-34, MMH-109-05, and MMH-114-80], the Ministry of Science and Technology, Taiwan [grant number MOST-109-2314-B-195-023], the National Science and Technology Council, Taiwan [grant numbers NSTC 112-2321-B-195-001-, NSTC 114-2321-B-195-001-, and NSTC 115-2321-B-195-001-], and Ministry of Health and Welfare, Taiwan [grant number HTS-114-115-A1-0006].

Institutional Review Board Statement: This study was conducted in accordance with the Declaration of Helsinki. The study protocol was approved by the Institutional Review Board of MacKay Memorial Hospital (Approval numbers: 18MMHIS050, Approval date: 22 August 2018; Approval numbers: 21MMHIS069e, Approval date: 20 April 2021).

Informed Consent Statement: Samples were collected after obtaining written informed consent from all participants, in compliance with the approved study protocol.

Data Availability Statement: The datasets generated and analyzed during the present study are available from the corresponding author on reasonable request. TCGA-BRCA data are publicly available from the Genomic Data Commons.

Conflicts of Interest: The authors declare no conflicts of interest.

References

1. Siegel, R.L.; Miller, K.D.; Fuchs, H.E.; Jemal, A. Cancer statistics, 2022. *CA Cancer J. Clin.* **2022**, *72*, 7–33. [CrossRef] [PubMed]
2. Nelson, D.R.; Brown, J.; Morikawa, A.; Method, M. Breast cancer-specific mortality in early breast cancer as defined by high-risk clinical and pathologic characteristics. *PLoS ONE* **2022**, *17*, e0264637. [CrossRef] [PubMed]
3. Wolf, N.K.; Kissiov, D.U.; Raulet, D.H. Roles of natural killer cells in immunity to cancer, and applications to immunotherapy. *Nat. Rev. Immunol.* **2023**, *23*, 90–105. [CrossRef] [PubMed]
4. Santos, E.M.; Rodrigues de Matos, F.; Freitas de Morais, E.; Galvão, H.C.; de Almeida Freitas, R. Evaluation of Cd8+ and natural killer cells defense in oral and oropharyngeal squamous cell carcinoma. *J. Cranio-Maxillofac. Surg.* **2019**, *47*, 676–681. [CrossRef] [PubMed]
5. Stabile, H.; Fionda, C.; Gismondi, A.; Santoni, A. Role of Distinct Natural Killer Cell Subsets in Anticancer Response. *Front. Immunol.* **2017**, *8*, 293. [CrossRef] [PubMed]
6. Su, Y.W.; Huang, W.Y.; Lin, S.H.; Yang, P.S. Effects of Reishimmune-S, a Fungal Immunomodulatory Peptide Supplement, on the Quality of Life and Circulating Natural Killer Cell Profiles of Patients With Early Breast Cancer Receiving Adjuvant Endocrine Therapy. *Integr. Cancer Ther.* **2024**, *23*, 15347354241242120. [CrossRef] [PubMed]
7. Mamessier, E.; Sylvain, A.; Thibult, M.L.; Houvenaeghel, G.; Jacquemier, J.; Castellano, R.; Gonçalves, A.; André, P.; Romagné, F.; Thibault, G.; et al. Human breast cancer cells enhance self tolerance by promoting evasion from NK cell antitumor immunity. *J. Clin. Investig.* **2011**, *121*, 3609–3622. [CrossRef] [PubMed]
8. Shabrish, S.; Gupta, M.; Madkaikar, M. A Modified NK Cell Degranulation Assay Applicable for Routine Evaluation of NK Cell Function. *J. Immunol. Res.* **2016**, *2016*, 3769590. [CrossRef] [PubMed]
9. Sivori, S.; Vacca, P.; Del Zotto, G.; Munari, E.; Mingari, M.C.; Moretta, L. Human NK cells: Surface receptors, inhibitory checkpoints, and translational applications. *Cell. Mol. Immunol.* **2019**, *16*, 430–441. [CrossRef] [PubMed]
10. Onkar, S.S.; Carleton, N.M.; Lucas, P.C.; Bruno, T.C.; Lee, A.V.; Vignali, D.A.A.; Oesterreich, S. The Great Immune Escape: Understanding the Divergent Immune Response in Breast Cancer Subtypes. *Cancer Discov.* **2023**, *13*, 23–40. [CrossRef] [PubMed]

11. Verma, R.; Hanby, A.M.; Horgan, K.; Verghese, E.T.; Volpato, M.; Carter, C.R.; Hughes, T.A. Levels of different subtypes of tumour-infiltrating lymphocytes correlate with each other, with matched circulating lymphocytes, and with survival in breast cancer. *Breast Cancer Res. Treat.* **2020**, *183*, 49–59. [CrossRef] [PubMed]
12. Chen, J.; Verdiell, A.; Formoso, C.; Luciano, M.; Chen, C.; Thakur, A. Tumor-derived extracellular vesicles: Bridging communication and next-generation theranostics. *Biomed. Pharmacother.* **2025**, *193*, 118815. [CrossRef] [PubMed]
13. Liu, Z.; Ding, M.; Qiu, P.; Pan, K.; Guo, Q. Natural killer cell-related prognostic risk model predicts prognosis and treatment outcomes in triple-negative breast cancer. *Front. Immunol.* **2023**, *14*, 1200282. [CrossRef] [PubMed]
14. Thacker, G.; Henry, S.; Nandi, A.; Debnath, R.; Singh, S.; Nayak, A.; Susnik, B.; Boone, M.M.; Zhang, Q.; Kesmodel, S.B.; et al. Immature natural killer cells promote progression of triple-negative breast cancer. *Sci. Transl. Med.* **2023**, *15*, eabl4414. [CrossRef] [PubMed]
15. Marcelin, H.N.; Dasse, R.S.; Yeboah, R.O.; Tariam, A.D.; Kagambega, A.G.Z.; Oseni, A.M.; Kouassi, Y.K.K.; Bilé, M.A.; Toure, M.; Thakar, M.; et al. Circulating natural killer cells and their association with breast cancer and its clinico-pathological characteristics. *Ecancermedicalscience* **2023**, *17*, 1567. [CrossRef] [PubMed]
16. Amin, M.B.; Greene, F.L.; Edge, S.B.; Compton, C.C.; Gershenwald, J.E.; Brookland, R.K.; Meyer, L.; Gress, D.M.; Byrd, D.R.; Winchester, D.P. The Eighth Edition AJCC Cancer Staging Manual: Continuing to build a bridge from a population-based to a more "personalized" approach to cancer staging. *CA Cancer J. Clin.* **2017**, *67*, 93–99. [CrossRef] [PubMed]
17. Yang, T.L.; Tsai, C.H.; Su, Y.W.; Chang, Y.C.; Lee, F.; Huang, T.Y.; Li, F.Y.; Yang, P.S. Combining *KPNA2* and *FOXM1* Expression as Prognostic Markers and Therapeutic Targets in Hormone Receptor-Positive, HER2-Negative Breast Cancer. *Cancers* **2025**, *17*, 671. [CrossRef] [PubMed]
18. Kim, D.; Paggi, J.M.; Park, C.; Bennett, C.; Salzberg, S.L. Graph-based genome alignment and genotyping with HISAT2 and HISAT-genotype. *Nat. Biotechnol.* **2019**, *37*, 907. [CrossRef] [PubMed]
19. Kovaka, S.; Zimin, A.V.; Pertea, G.M.; Razaghi, R.; Salzberg, S.L.; Pertea, M. Transcriptome assembly from long-read RNA-seq alignments with StringTie2. *Genome Biol.* **2019**, *20*, 278. [CrossRef] [PubMed]
20. Ritchie, M.E.; Phipson, B.; Wu, D.; Hu, Y.; Law, C.W.; Shi, W.; Smyth, G.K. limma powers differential expression analyses for RNA-sequencing and microarray studies. *Nucleic Acids Res.* **2015**, *43*, e47. [CrossRef] [PubMed]
21. Chen, Y.; Chen, L.; Lun, A.T.L.; Baldoni, P.L.; Smyth, G.K. edgeR v4: Powerful differential analysis of sequencing data with expanded functionality and improved support for small counts and larger datasets. *Nucleic Acids Res.* **2025**, *53*, gkaf018. [CrossRef] [PubMed]
22. Xu, S.; Hu, E.; Cai, Y.; Xie, Z.; Luo, X.; Zhan, L.; Tang, W.; Wang, Q.; Liu, B.; Wang, R.; et al. Using clusterProfiler to characterize multiomics data. *Nat. Protoc.* **2024**, *19*, 3292–3320. [CrossRef] [PubMed]
23. Mazumdar, M.; Glassman, J.R. Categorizing a prognostic variable: Review of methods, code for easy implementation and applications to decision-making about cancer treatments. *Stat. Med.* **2000**, *19*, 113–132. [CrossRef]
24. Conte, B.; Brasó-Maristany, F.; Hernández, A.R.; Pascual, T.; Villacampa, G.; Schettini, F.; Vidal Losada, M.J.; Seguí, E.; Angelats, L.; Garcia-Fructuoso, I.; et al. A 14-gene B-cell immune signature in early-stage triple-negative breast cancer (TNBC): A pooled analysis of seven studies. *eBioMedicine* **2024**, *102*, 105043. [CrossRef] [PubMed]
25. Lorenzo-Herrero, S.; Sordo-Bahamonde, C.; Gonzalez, S.; López-Soto, A. CD107a Degranulation Assay to Evaluate Immune Cell Antitumor Activity. *Methods Mol. Biol.* **2019**, *1884*, 119–130. [CrossRef] [PubMed]
26. Schmid, P.; Cortes, J.; Pusztai, L.; McArthur, H.; Kümmel, S.; Bergh, J.; Denkert, C.; Park, Y.H.; Hui, R.; Harbeck, N.; et al. Pembrolizumab for Early Triple-Negative Breast Cancer. *N. Engl. J. Med.* **2020**, *382*, 810–821. [CrossRef] [PubMed]
27. Loi, S.; Salgado, R.; Curigliano, G.; Romero Díaz, R.I.; Delaloge, S.; Rojas García, C.I.; Kok, M.; Saura, C.; Harbeck, N.; Mittendorf, E.A.; et al. Neoadjuvant nivolumab and chemotherapy in early estrogen receptor-positive breast cancer: A randomized phase 3 trial. *Nat. Med.* **2025**, *31*, 433–441. [CrossRef] [PubMed]
28. Cardoso, F.; O'Shaughnessy, J.; Liu, Z.; McArthur, H.; Schmid, P.; Cortes, J.; Harbeck, N.; Telli, M.L.; Cescon, D.W.; Fasching, P.A.; et al. Pembrolizumab and chemotherapy in high-risk, early-stage, $ER^{+}/HER2^{-}$ breast cancer: A randomized phase 3 trial. *Nat. Med.* **2025**, *31*, 442–448. [CrossRef] [PubMed]
29. Chen, N.; Higashiyama, N.; Hoyos, V. Predictive Biomarkers of Immune Checkpoint Inhibitor Response in Breast Cancer: Looking beyond Tumoral PD-L1. *Biomedicines* **2021**, *9*, 1863. [CrossRef] [PubMed]
30. Li, M.; Panet, F.; Barberi, V.; Salgado, R.; Oliveira, M.; Loi, S. Biomarkers of response and resistance to immune checkpoint inhibitors in breast cancer. *Breast* **2025**, *83*, 104545. [CrossRef] [PubMed]
31. Kos, Z.; Roblin, E.; Kim, R.S.; Michiels, S.; Gallas, B.D.; Chen, W.; van de Vijver, K.K.; Goel, S.; Adams, S.; Demaria, S.; et al. Pitfalls in assessing stromal tumor infiltrating lymphocytes (sTILs) in breast cancer. *npj Breast Cancer* **2020**, *6*, 17. [CrossRef] [PubMed]
32. Loi, S.; Drubay, D.; Adams, S.; Pruneri, G.; Francis, P.A.; Lacroix-Triki, M.; Joensuu, H.; Dieci, M.V.; Badve, S.; Demaria, S.; et al. Tumor-Infiltrating Lymphocytes and Prognosis: A Pooled Individual Patient Analysis of Early-Stage Triple-Negative Breast Cancers. *J. Clin. Oncol.* **2019**, *37*, 559–569. [CrossRef] [PubMed]

33. Dieci, M.V.; Conte, P.; Bisagni, G.; Brandes, A.A.; Frassoldati, A.; Cavanna, L.; Musolino, A.; Giotta, F.; Rimanti, A.; Garrone, O.; et al. Association of tumor-infiltrating lymphocytes with distant disease-free survival in the ShortHER randomized adjuvant trial for patients with early HER2+ breast cancer. *Ann. Oncol.* **2019**, *30*, 418–423. [CrossRef] [PubMed]
34. Solinas, C.; Ceppi, M.; Lambertini, M.; Scartozzi, M.; Buisseret, L.; Garaud, S.; Fumagalli, D.; de Azambuja, E.; Salgado, R.; Sotiriou, C.; et al. Tumor-infiltrating lymphocytes in patients with HER2-positive breast cancer treated with neoadjuvant chemotherapy plus trastuzumab, lapatinib or their combination: A meta-analysis of randomized controlled trials. *Cancer Treat. Rev.* **2017**, *57*, 8–15. [CrossRef] [PubMed]
35. Loi, S.; Sirtaine, N.; Piette, F.; Salgado, R.; Viale, G.; Van Eenoo, F.; Rouas, G.; Francis, P.; Crown, J.P.; Hitre, E.; et al. Prognostic and predictive value of tumor-infiltrating lymphocytes in a phase III randomized adjuvant breast cancer trial in node-positive breast cancer comparing the addition of docetaxel to doxorubicin with doxorubicin-based chemotherapy: BIG 02-98. *J. Clin. Oncol.* **2013**, *31*, 860–867. [CrossRef] [PubMed]
36. Xue, J.S.; Ding, Z.N.; Meng, G.X.; Yan, L.J.; Liu, H.; Li, H.C.; Yao, S.Y.; Tian, B.W.; Dong, Z.R.; Chen, Z.Q.; et al. The Prognostic Value of Natural Killer Cells and Their Receptors/Ligands in Hepatocellular Carcinoma: A Systematic Review and Meta-Analysis. *Front. Immunol.* **2022**, *13*, 872353. [CrossRef] [PubMed]
37. Angelats, L.; Paré, L.; Rubio-Perez, C.; Sanfeliu, E.; González, A.; Seguí, E.; Villacampa, G.; Marín-Aguilera, M.; Pernas, S.; Conte, B.; et al. Linking tumor immune infiltration to enhanced longevity in recurrence-free breast cancer. *ESMO Open* **2025**, *10*, 104109. [CrossRef] [PubMed]
38. Alim, L.F.; Keane, C.; Souza-Fonseca-Guimaraes, F. Molecular mechanisms of tumour necrosis factor signalling via TNF receptor 1 and TNF receptor 2 in the tumour microenvironment. *Curr. Opin. Immunol.* **2024**, *86*, 102409. [CrossRef] [PubMed]
39. He, D.; Li, H.; Yusuf, N.; Elmets, C.A.; Li, J.; Mountz, J.D.; Xu, H. IL-17 promotes tumor development through the induction of tumor promoting microenvironments at tumor sites and myeloid-derived suppressor cells. *J. Immunol.* **2010**, *184*, 2281–2288. [CrossRef] [PubMed]
40. Zalfa, C.; Paust, S. Natural Killer Cell Interactions With Myeloid Derived Suppressor Cells in the Tumor Microenvironment and Implications for Cancer Immunotherapy. *Front. Immunol.* **2021**, *12*, 633205. [CrossRef] [PubMed]
41. Tufail, M.; Jiang, C.H.; Li, N. Immune evasion in cancer: Mechanisms and cutting-edge therapeutic approaches. *Signal Transduct. Target. Ther.* **2025**, *10*, 227. [CrossRef] [PubMed]
42. Vallée, A.; Lecarpentier, Y. Crosstalk Between Peroxisome Proliferator-Activated Receptor Gamma and the Canonical WNT/β-Catenin Pathway in Chronic Inflammation and Oxidative Stress During Carcinogenesis. *Front. Immunol.* **2018**, *9*, 745. [CrossRef] [PubMed]
43. Su, Y.-W. Menopause, Aged Fat Cells and Adipocyte Dysfunction. *Int. J. Gerontol.* **2025**, *19*, 4–5.
44. Zhao, B.; Xin, Z.; Ren, P.; Wu, H. The Role of PPARs in Breast Cancer. *Cells* **2022**, *12*, 130. [CrossRef] [PubMed]
45. Cui, M.; Huang, J.; Zhang, S.; Liu, Q.; Liao, Q.; Qiu, X. Immunoglobulin Expression in Cancer Cells and Its Critical Roles in Tumorigenesis. *Front. Immunol.* **2021**, *12*, 613530. [CrossRef] [PubMed]
46. Almeida-Oliveira, A.; Smith-Carvalho, M.; Porto, L.C.; Cardoso-Oliveira, J.; Ribeiro Ados, S.; Falcão, R.R.; Abdelhay, E.; Bouzas, L.F.; Thuler, L.C.; Ornellas, M.H.; et al. Age-related changes in natural killer cell receptors from childhood through old age. *Hum. Immunol.* **2011**, *72*, 319–329. [CrossRef] [PubMed]
47. Fionda, C.; Ruggeri, S.; Sciumè, G.; Laffranchi, M.; Quinti, I.; Milito, C.; Palange, P.; Menichini, I.; Sozzani, S.; Frati, L.; et al. Age-dependent NK cell dysfunctions in severe COVID-19 patients. *Front. Immunol.* **2022**, *13*, 1039120. [CrossRef] [PubMed]

Disclaimer/Publisher's Note: The statements, opinions and data contained in all publications are solely those of the individual author(s) and contributor(s) and not of MDPI and/or the editor(s). MDPI and/or the editor(s) disclaim responsibility for any injury to people or property resulting from any ideas, methods, instructions or products referred to in the content.